

Supplemental Information: Oxidative instability of ionomers in hydroxide-exchange-membrane electrolyzers

Grace A. Lindquist, Jamie C. Gaitor, Willow L. Thompson,
Valerie Brogden, Kevin J. T. Noonan, and Shannon W. Boettcher*

G. A. L., W. L. T., V. B., and S. W. B.
Department of Chemistry and Biochemistry
and the Oregon Center for Electrochemistry
University of Oregon
Eugene, Oregon 97403, USA
*E-mail: swb@uoregon.edu

J. C. G. and K. J. T. N.
Department of Chemistry
Carnegie Mellon University
Pittsburgh, Pennsylvania 15213-2617, USA
E-mail: noonan@andrew.cmu.edu

Supplemental Information

PNB ionomer conductivity, ion exchange capacity (IEC), and water uptake (WU).
Conductivity was measured by four-probe electrochemical impedance spectroscopy (EIS) using a Scribner Membrane Conductivity Clamp and a Bio-Logic SP-150 Potentiostat as in our prior reports.¹⁻³ IEC was measured using standard back-titration methods and carried out according to our prior reports.¹⁻³ The material was in the Cl⁻ form after IEC analysis, and all manipulations for membrane electrode assembly fabrication were carried out on the membrane with a Cl⁻ counterion. Water uptake was determined using the following equation:

$$\text{WU (\%)} = \frac{M_w - M_d}{M_d} \times 100$$

Where M_w = mass of hydrated film in ⁻OH form and M_d = mass of the dry film in the ⁻Cl form.

Detailed description of electrolyzer assembly with integrated reference electrode. As described in the main body text, a reference electrode is integrated in the MEA by extending a strip of membrane outside the electrolyzer hardware and attaching a Hg/HgO reference electrode submerged in KOH. For assembly, the anode PTE is placed on the anode flow field with the appropriate number of gaskets (Fig. S3). Next, a support gasket is added and the membrane strip is placed across the flow field so the edge is touching the edge of the anode PTE (Fig. S4). The gasket under the membrane strip has a tab that extends outside the electrolyzer hardware to support the membrane strip and isolate the strip from contacting the flow field (Fig. S5). Then, a thinner gasket is placed on top of the membrane strip (Fig. S6). This gasket has a slit cut in the tab to act as a water channel and help maintain water flow to the membrane strip (Fig. S7). After, the HEM is placed on top of the anode PTE, overlapping with the membrane strip (Fig. S8). Another isolation gasket (Fig. S5) is placed on top of the stack to keep the strip from touching the cathode flow field (Fig. S9). The cathode PTE is then placed on top of the AEM and stacked with the remaining gaskets (Fig. S10). Schematics of the regular and reference electrode MEAs are shown in Fig. S11.

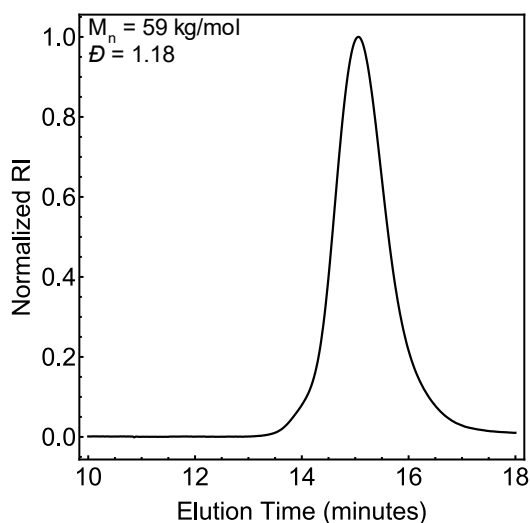


Figure S1. GPC trace of 60:40 NB-5-Hex-co-NB-5-BuBr copolymer.

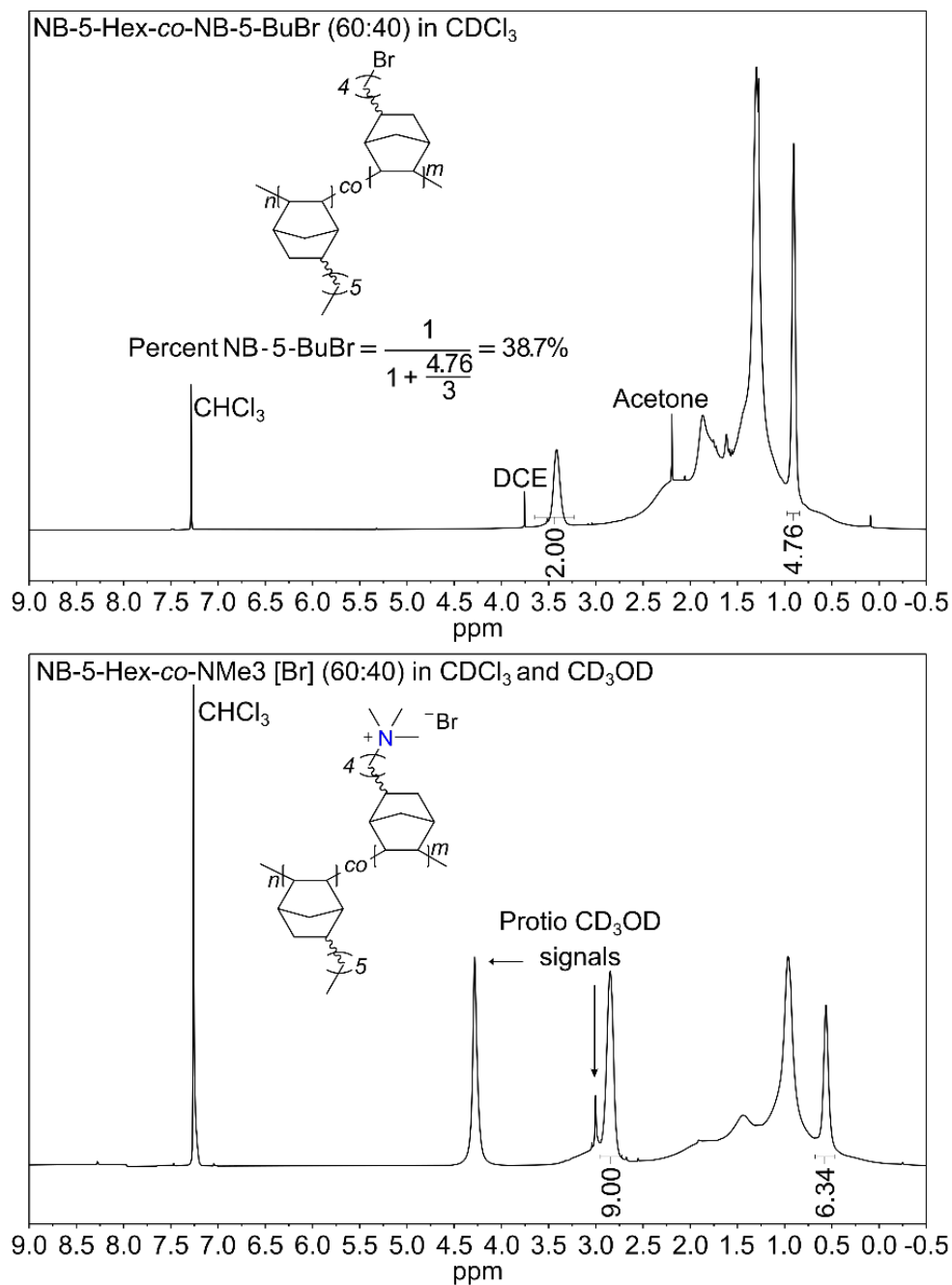


Figure S2. ¹H NMR spectra (500 MHz) of DP 500 60:40 NB-5-Hex-co-NB-5-BuBr copolymer before (Top) and after (Bottom) NMe₃ substitution, collected in 1:1 CDCl₃:CD₃OD. A 9:4.5 ratio should be observed for the N-methyl groups of the trimethylammonium to the terminal methyl group from the hexyl chain of the NB-5-Hex for a 40 mol% ionic copolymer.

Table S1 Membrane properties for the hydroxide exchange polymers used in this study.

	Water uptake (%)	$\sigma_{22\text{ }^\circ\text{C}} \text{OH}^-$ (mS/cm)	Ion exchange capacity (mmol/g)	λ
60:40 NB-5-Hex-co-NMe ₃	88	45 ± 3	1.91	26
PiperION TP-85 ⁴	46	80 ± 5	2.30-2.37	N/A



Figure S3. Anode PTE on the anode flow field

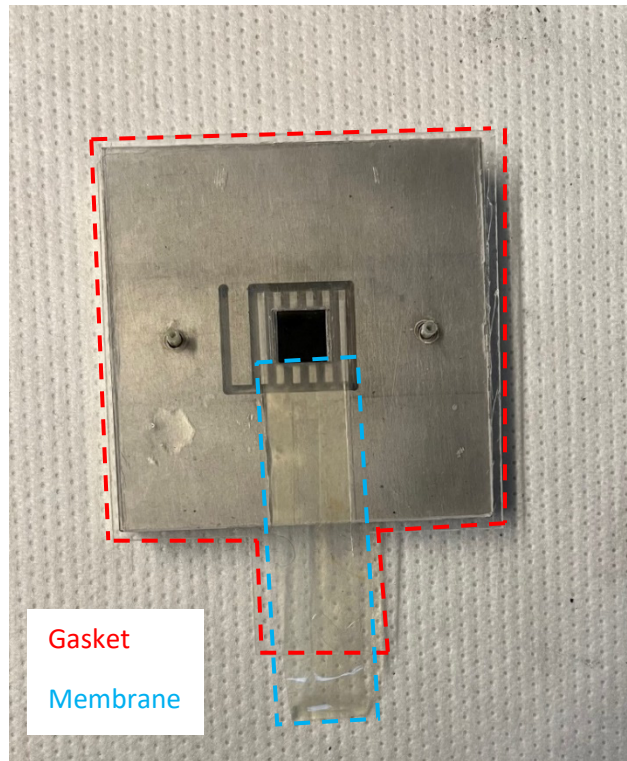


Figure S4. membrane strip placed on the support gasket and aligned at the edge of the anode PTE.

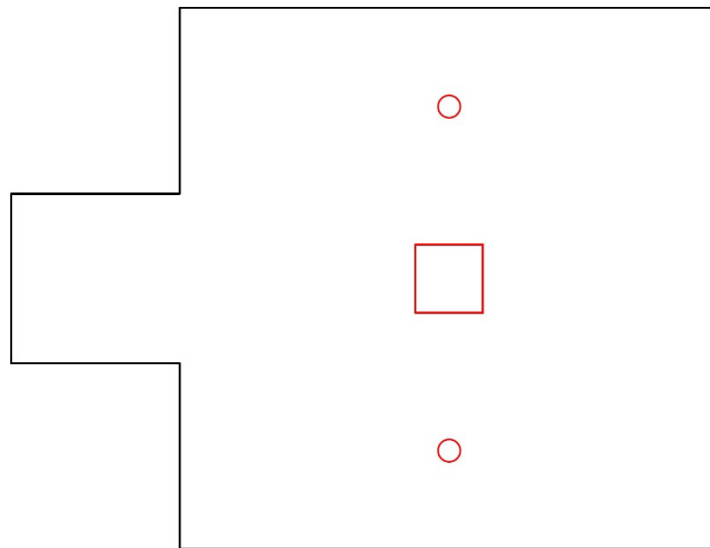


Figure S5. Shape of gasket used under and above the membrane strip.

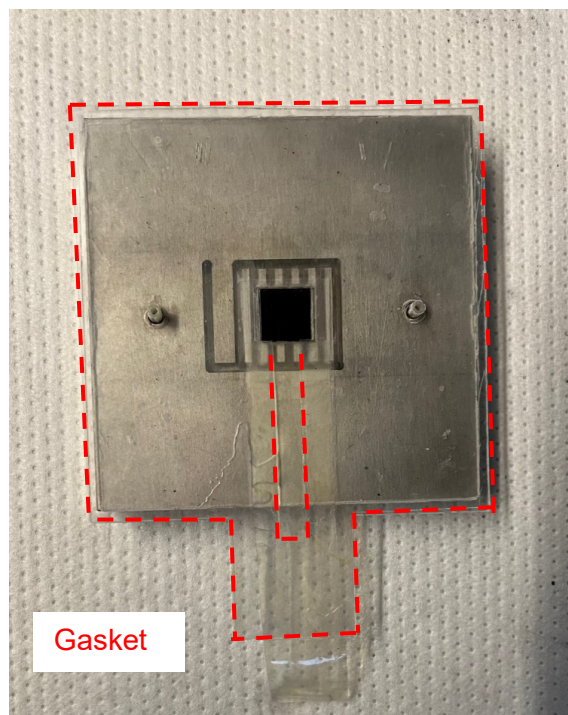


Figure S6. Gasket with water channel placed on top of membrane strip.

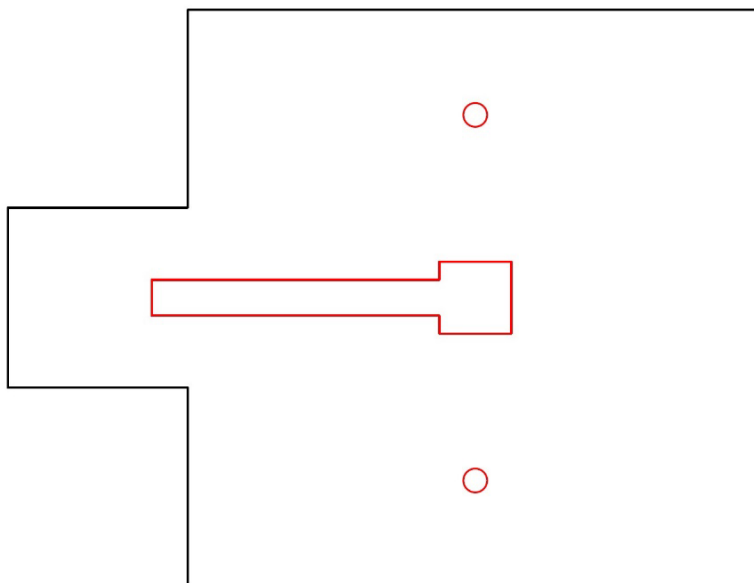


Figure S7. Shape of gasket with water channel.

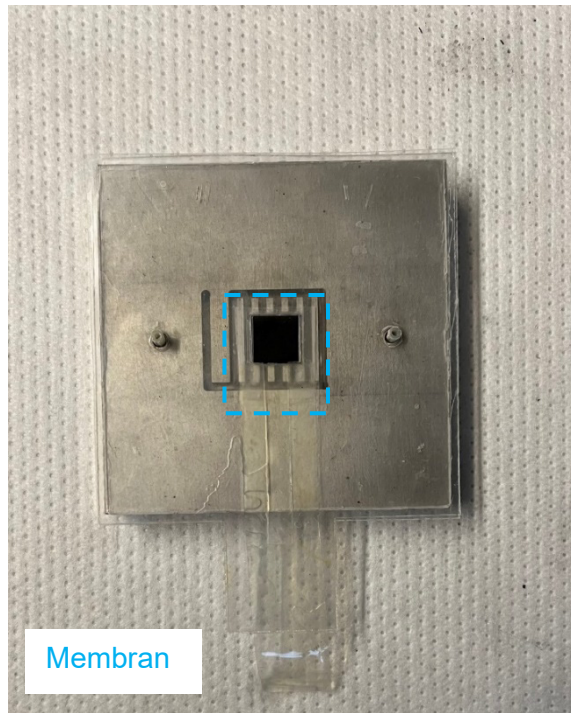


Figure S8. AEM placed on top of the anode PTE. The AEM is cut wide enough to overlap with the membrane strip past the outer edge of the serpentine pattern.

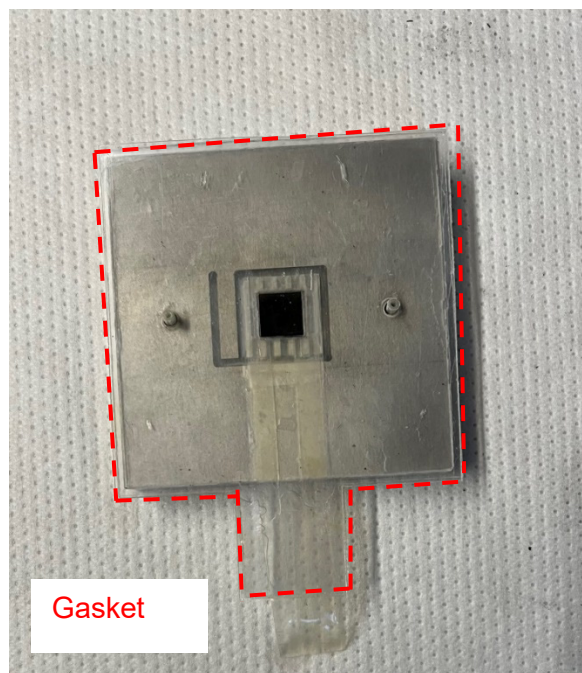


Figure S9. Another isolation gasket is placed on top of the stack.



Figure S10. Cathode PTE placed on top of the AEM, completing the MEA.

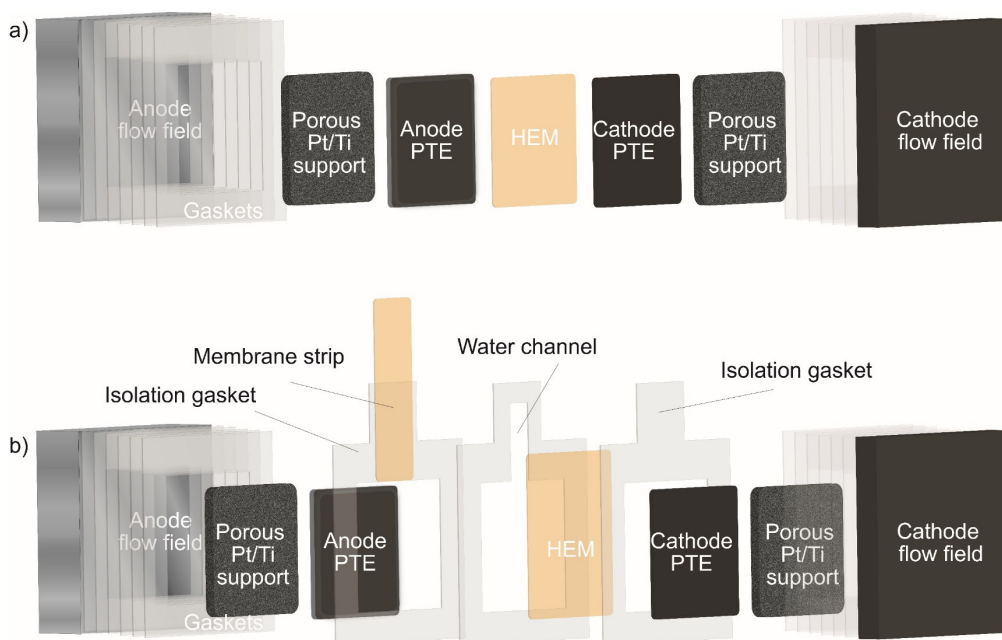


Figure S11. Schematic of MEA components. a) standard MEA and b) MEA with integrated reference electrode. The membrane used was the PiperION TP-85 and cathode catalyst layer Pt black with TP-85 ionomer for all AEM studies.

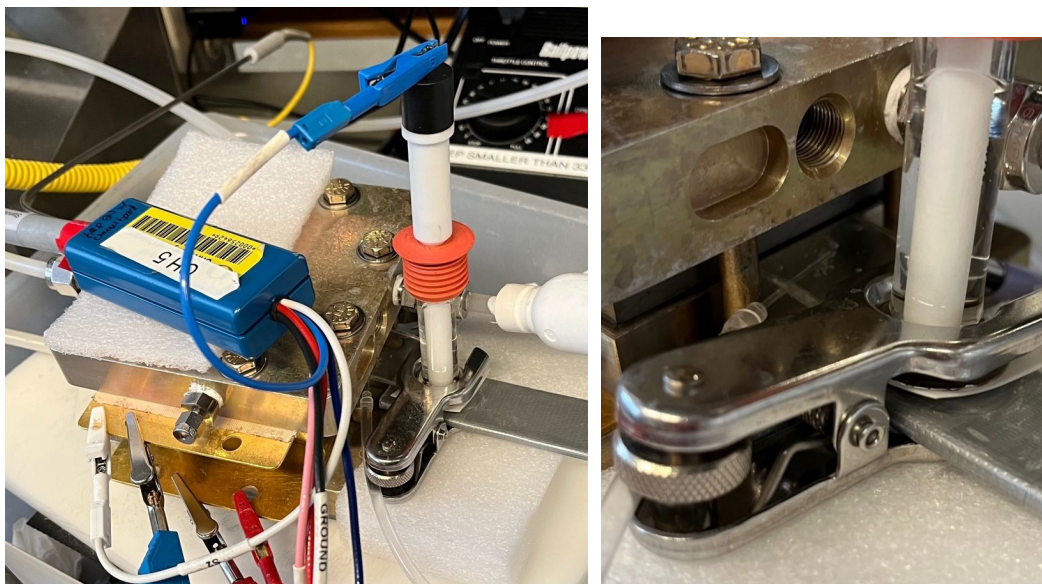


Figure S12. Photos of electrolyzer hardware with reference electrode and close-up of strip with gaskets isolating contact with the flow fields. A water drip is clamped between the membrane strip gaskets to keep the membrane hydrated. A Schlenk line adapter is clamped to the membrane strip and filled with 0.1 M KOH. The Hg/HgO reference electrode is submerged in electrolyte.

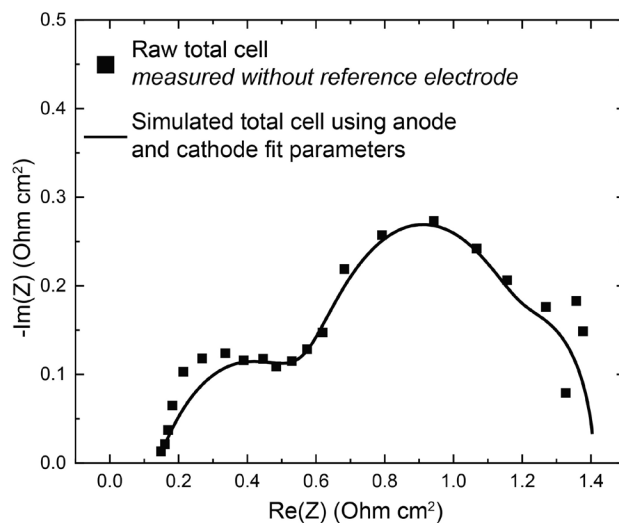


Figure S13. Comparison of total cell impedance with and without reference electrode. The fit parameters obtained from the anode and cathode Nyquist plots were used to simulate the total cell impedance (line). The data agrees well with the raw total cell impedance measured without the reference electrode (points). Error in the high frequency region is due to high error from the anode signal, as the anode cannot be resolved above ~ 600 Hz due to a potentiostat limitation. *This data demonstrates the accuracy of the reference cell impedance in separating the individual electrode impedances.*

Table S2: EIS fit parameters for full cell data in Figure 3c. The data was fit using three RC circuit components as informed by the reference electrode data. One RC component for each fit does not contribute substantially (highlighted values).

Time (h)	R1 (Ohm·cm ²)	Q2 (mF·s ^(α-1))	α2	R2 (Ohm·cm ²)	Q3 (mF·s ^(α-1))	α3	R3 (Ohm·cm ²)	Q4 (mF·s ^(α-1))	α4	R4 (Ohm·cm ²)
0	0.147	73	0.64	0.94	0.836	0.79	0.328	$3.6 \cdot 10^{-22}$	1	$4.34 \cdot 10^{-8}$
5	0.124	0.50	0.774	0.73	$4.08 \cdot 10^{-4}$	0.746	$1.55 \cdot 10^{-10}$	54	8.29E-01	0.832
10	0.075	0.22	0.75	1.2	43	0.75	1.016	$3.7 \cdot 10^{-7}$	$4.90 \cdot 10^{-5}$	$1.9 \cdot 10^{-16}$
15	0.083	0.055	0.85	1.1	27	0.725	1.264	$1.6 \cdot 10^{-12}$	0.56	$5.7 \cdot 10^{-03}$
20	0.09	0.087	0.8	1.2	$1.72 \cdot 10^{-18}$	$3.14 \cdot 10^{-4}$	$4.21 \cdot 10^{-7}$	0.2	7.90E-01	1.19

Table S3: EIS fit parameters for cathode measured with reference electrode in Figure 3d.

Time (h)	R1 (Ohm·cm ²)	Q2 (mF·s ^(α-1))	α2	R2 (Ohm·cm ²)
0	0.07	1074	1	0.178
20	0.078	739	0.901	0.241

Table S4: EIS fit parameters for anode measured with reference electrode in Figure 3d.

Time (h)	R1 (Ohm·cm ²)	Q2 (mF·s ^(α-1))	α2	R2 (Ohm·cm ²)	Q3 (mF·s ^(α-1))	α3	R3 (Ohm·cm ²)
0	0.07*	41	0.841	0.613	120	0.532	0.48
20	0.07*	131	0.795	0.566	260	0.525	1.67

*anode R1 was fixed to given value. The high frequency resistance is not resolvable for anode reference signal due to potentiostat limitations.

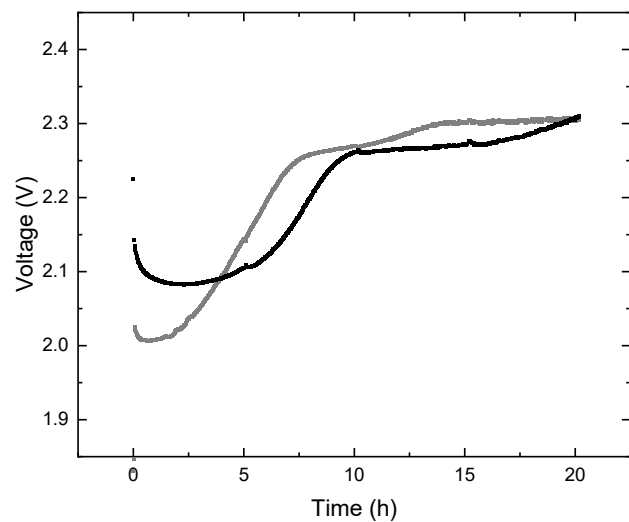


Figure S14. Comparison of HEM operation with 10% anode ionomer content (gray) and 20% anode ionomer content (black).

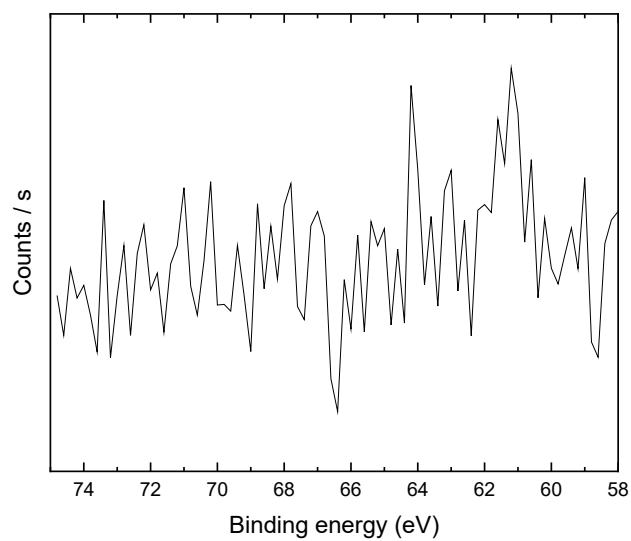


Figure S15. Ir 4f XPS region of a pristine TP-85 anode. Ir signal is blocked by the top ionomer coating.

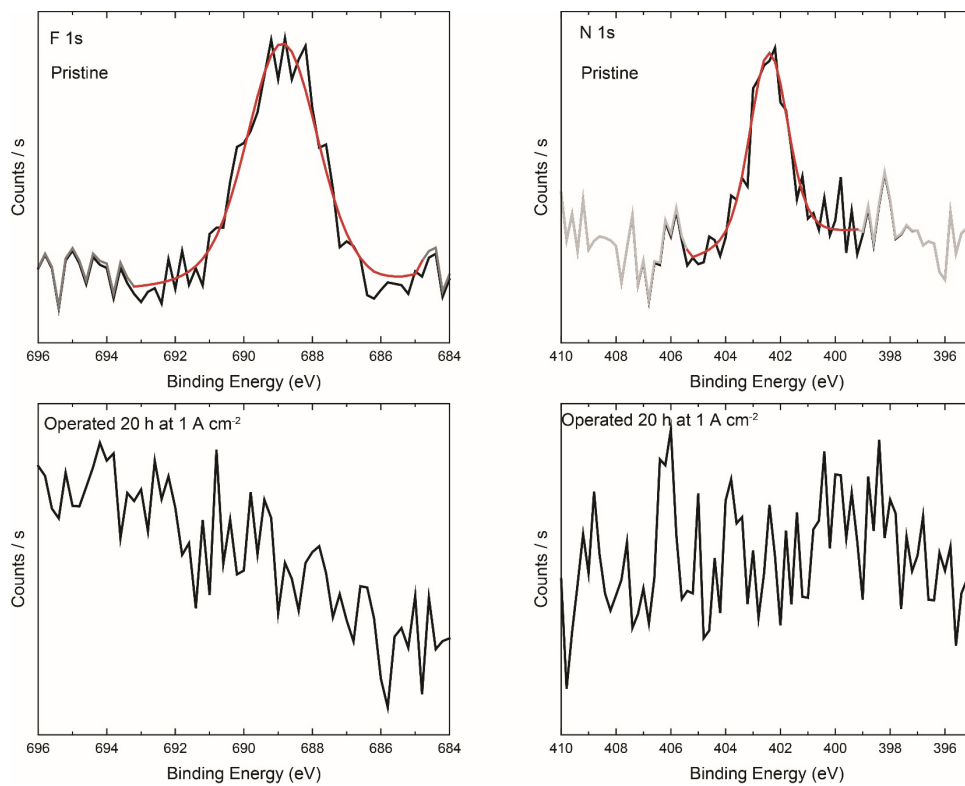


Figure S16. F 1s and N 1s XP spectra of pristine TP-85 anode PTE (top) and PTE after operated (bottom). All F and N content is no longer resolved.

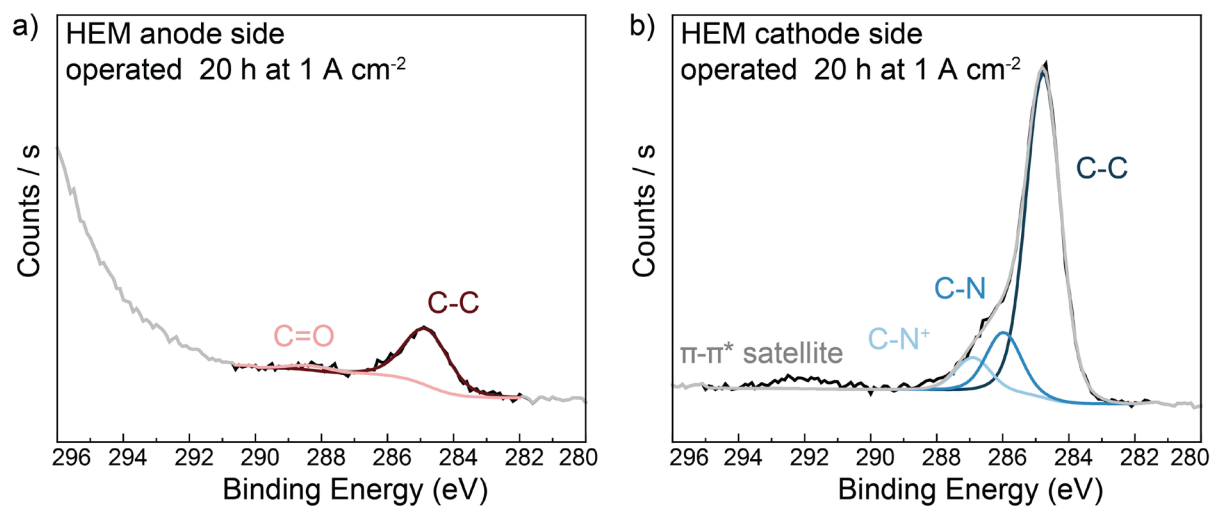


Figure S17. XPS comparison of a) anode and b) cathode side of a HEM. Cells were operated with an $\text{IrO}_x/\text{TP-85}$ catalyst layer on Pt/Ti PTL (anode), Pt-black/TP-85 catalyst layer on Toray carbon-paper PTL (cathode), and TP-85 membrane at 1 A cm^{-2} for 20 h.

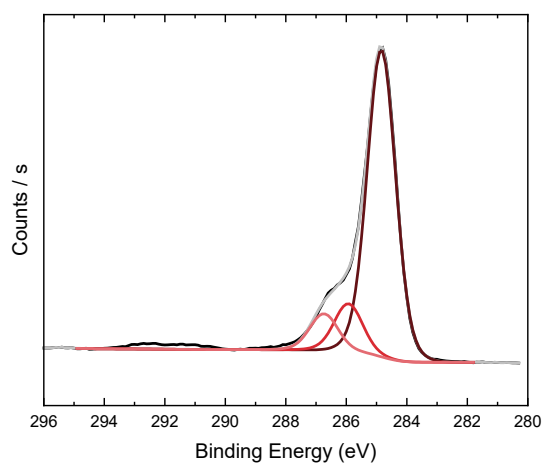


Figure S18. C 1s XPS of an $\text{IrO}_x/\text{TP-85}$ anode PTE after assembled in a device and operated with only water flow (no applied current/voltage) for 24 h.

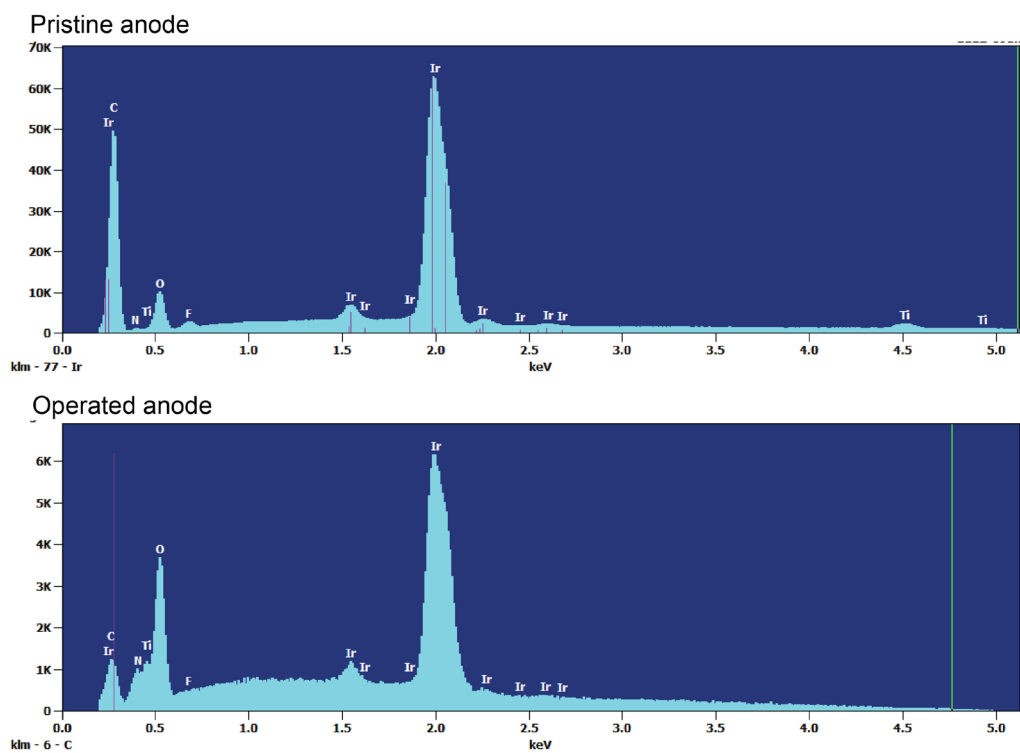


Figure S19: EDS counts of the a) pristine and b) operated anode. The operated anode shows a lower C signal and loss of F, consistent with XPS results.

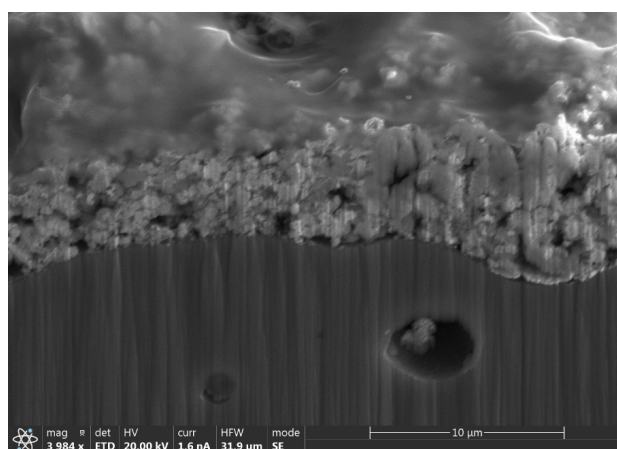


Figure S20. Cross section of an IrO_x/TP-85 anode PTE after assembled in a device and exposed to water flow at 70 °C (no applied current) for 24 h. The top ionomer layer and ionomer network throughout the catalyst layer are still intact.

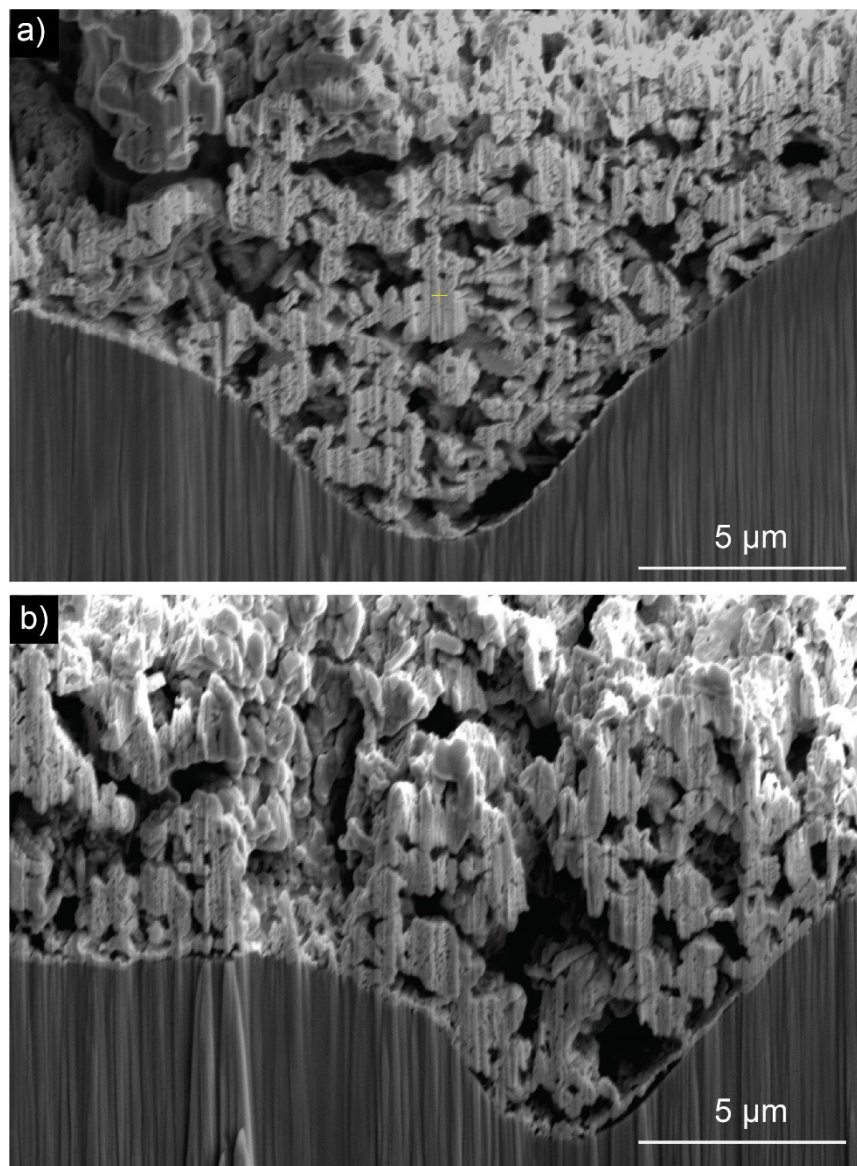


Fig. S21 Cross section of an IrO_x/Nafion anode after operation with a) PEM and b) HEM.

References

1. J. C. Gaitor, M. Treichel, T. Kowalewski and K. J. T. Noonan, *ACS Appl. Polym. Mater.*, 2022, **4**, 8032-8042.
2. M. Treichel, C. Tyler Womble, R. Selhorst, J. Gaitor, T. M. S. K. Pathiranaage, T. Kowalewski and K. J. T. Noonan, *Macromolecules*, 2020, **53**, 8509-8518.
3. R. Selhorst, J. Gaitor, M. Lee, D. Markovich, Y. Yu, M. Treichel, C. Olavarria Gallegos, T. Kowalewski, L. F. Kourkoutis, R. C. Hayward and K. J. T. Noonan, *ACS Appl. Energy Mater.*, 2021, **4**, 10273-10279.
4. J. Wang, Y. Zhao, B. P. Setzler, S. Rojas-Carbonell, C. Ben Yehuda, A. Amel, M. Page, L. Wang, K. Hu, L. Shi, S. Gottesfeld, B. Xu and Y. Yan, *Nat. Energ.*, 2019, **4**, 392-398.